International Journal on Recent and Innovation Trends in Computing and Communication
ISSN: 2321-8169 Volume: 10 Issue: 2s
DOI: https://doi.org/10.17762/ijritcc.v10i2s.5927
***Article Received**: 08 October 2022 **Revised**: 12 November 2022 **Accepted**: 22 December 2022*

Convolutional Gated Recurrent Neural Network Based Automatic Detection and Classification of Brain Tumor using Magnetic Resonance Imaging

[1]S. R. Sridhar, [2]Dr. M. Akila, [3]Dr. R. Asokan
[1]Department of Computer Science and Engineering, Muthayammal Engineering College
Namakkal, 637408, India,
Email: srsridharfz@gmail.com
[2]Department of Computer Science and Engineering, KPR Institute of Engineering and Technology
Coimbatore, 641407, India
Email:akila@nvgroup.in
[3]Department of Electronics and Communication Engineering, Kongunadu College of Engineering and Technology
Trichy, 621215, India
Email:asokece@gmail.com

Abstract—Magnetic Resonance Imaging (MRI) might be a problematic assignment for tumor fluctuation and complexity because of brain image classification. This work presents the brain tumor classification system using Convolutional Gated Recurrent Neural Network (CGRNN) algorithm based on MRI images. The proposed tumor recognition framework comprises of four stages, to be specific preprocessing, feature extraction, segmentation and classification. Extraction of identified tumor framework features was accomplished utilizing Gray Level Co-occurrence Matrix (GLCM) strategy. At long last, the Convolutional Gated Recurrent Neural Network Classifier has been created to perceive various kinds of brain disease. The proposed framework can be effective in grouping these models and reacting to any variation from the abnormality. The entire framework is isolated into different types of phases: the Learning/Training Phase and the Recognition/Test Phase. A CGRNN classifier under the scholarly ideal separation measurements is utilized to decide the chance of every pixel having a place with the foreground (tumor) and the background. MATLAB software is used in the development of the simulation of the proposed system. The suggested method's simulation results show that the analysis of brain tumours is stable. It shows that the proposed brain tumor classifications are superior to those from brain MRIs than existing brain tumor classifications. The overall accuracy of the proposed system is 98.45%.

Keywords-Malignant; Benign; Feature extraction; Segmentation; Recurrent network.

I. INTRODUCTION

The brain is moreover the base camp of the human focal sensory framework and the brain is an astounding organ that has an extraordinarily gigantic arrangement of 50-100 billion neurons. Normally tumor is a mix of cells that make around the cerebrum, either inside or outside. There are an assortment of brain tumors are accessible, for example, malignant and benign brain. It is less hurtful, all the more generally interpreted, and as a result of it its right reaction is spread to different pieces of the body and all around treated because of its appropriate reaction. A benign tumor is less unsafe s to dangerous tumors. Malignant tumors are hurtful turns of events. Most of the time block therapists can spread the various bits of the body. The malignant tumors are labeled as the base and sub-tumors.

The fast malignant tumor spreads and attacks other brain tissues and debilitates the health condition, which in no time leads to a significant share. Premature judgment is the most experimental issue in the brain's unexpected systemic examination as a result of the emergence of brain tumors [1-4]. Brain tumor detection techniques, image segmentation structures accept an essentialness task in order to free MRI images. MRI comes in the form of image segmentation, for example it offers two types of lower-level information about delicate brain tissues. A manual as well as MRI brain image segmentation With respect to malignancy, brain tumors are physically produced using segmentation MRI images, comprising of a lot of information created in the clinical daily schedule, which is a tedious and testing task. At that point, programmed brain tumor image segmentation is required. As of late, profound learning strategies for mechanized investigation have gotten mainstream if these techniques can take care of the issue in a propelled manner to accomplish improved outcomes [5].

The actual segmentation time is similarly difficult to achieve, yet the medical practice does not attract a couple of moments of computation time. Another basic angle that requires brain tumor segmentation strategies is steadiness.

International Journal on Recent and Innovation Trends in Computing and Communication
ISSN: 2321-8169 Volume: 10 Issue: 2s
DOI: https://doi.org/10.17762/ijritcc.v10i2s.5927
***Article Received**: 08 October 2022 **Revised**: 12 November 2022 **Accepted**: 22 December 2022*

Each new technique used in clinical practice has become one of the most important evaluation models. Some current brain tumor segmentation procedures give extraordinary results in wonderful computational time [7]. Along these lines in this research work proposed, a Convolutional Gated Recurrent Neural Network Classifier has been created to perceive various sorts of brain diseases. The proposed framework was discovered effective in the classification of these examples and reacted to any variation of abnormality.

II. Literature Survey

An advanced magnetic resonance imaging (MRI) architectures contains tensor imaging (DTI), MR spectrometry (MS) and a pair of surface MRIs [8-9]. Brain tumor is extensively portrayed into two sorts: hurtful tumors (malignant) and noncancerous tumors (benign). The World Health Organization (WHO) is divided the tumor from four types such as, grade I to IV [10]. Cucumber cell astrocytoma is the name given to Grade I tumours. Anaplastic astrocytoma is a Grade II tumour, below average astrocytoma is a Grade III tumour, and glioblastomas are a Grade IV tumour. [11].

Analyzing procedures with image processing are essential precursors and obtained the brain tissue from MRI images [12]. The evaluation of malignant growth of the ligament in the tumor area is a significant task for the evaluation of therapeutic and therapeutic outcomes. A different types of semi-robotized and automated methods are used for brain image segmentation [13]. The MRI brain simulation system has a variety of projects that are used to analyze the brain, including T1 mass (TI) and T1 weighted merit improvement (T1c stage), T2 mass, and T2 tumor recovery (flare) approaches, building structures and reducing fluid mass. The different features used by X-pillar brain tumor segmentation include the adjacent map [15], including the image surface [14], and the assist characteristic, Eagan [16].

The Random Forests and Support Vector Machines (SVMs) based machine learning strategies are investigate MRI brain tumor segmentation and classification [17]. Deep learning development and procedures are the standard for analyzing our brain tumor segmentation during the field of image preprocessing, MRI image brain segmentation and MRI brain tumor classification. Further, the deep learning procedures have increased top-level execution for assessment of cerebrum tumors by various model MRIs. Convolutional Neural Network (CNN) system is a marvelous strategy that has got image stability and desire. In any case, the use of brain tumor classification and follow-up time is an indicator for patients who have a CNN habit. The deep learning techniques that are used in classification assessment introduced by tumors are de-noising auto encoders that are controlled by the stacked strings and the Convolutional Boltzmann machine. Based on the performance of all deep learning techniques, the Two-dimensional and three dimensional Convolutional Neural Networks are achieve the best result. The image blocks of the segmentation technique are arranged into various classes, for example, corruption, solid tissue, edema, upgraded center and non-improved center [18-23]

III. Materials And Method

The use of MRI for detect brain tumours is a subject of growing interest of brain tissue and tumour segmentation. It makes use of an automated technique as well as textural characteristics to identify the blocks of each nerve in the brain MRI region, among other things.

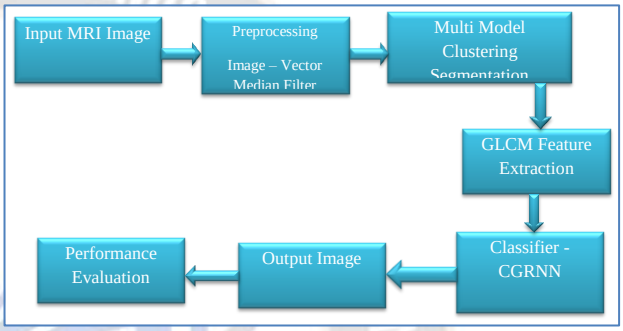

Figure 1: Block Diagram of Proposed System

Preprocessing, segmentation, and classification of brain pictures are among the phases in the proposed automated brain tumour detection algorithm. The Convolutional Gated Recurrent Neural Network-based brain tumor discovery and classification framework is appeared in Figure 1. The proposed tumor recognition framework comprises of four stages, to be specific preprocessing, feature extraction, segmentation and classification. The exploration work will be clarified in the accompanying sections.

3.1 Preprocessing Vector Median Filter

The preprocessing of MRI brain images is a stage that must require the proposed strategy to dispense with noise. The preprocessed image is done to limit the noise and to additionally upgrade the capacity in the info image. The motivation behind these pre-handling is fundamentally to improve the image quality so as to acquire more noteworthy lucidity and facilitate the recognition of tumors.

Step 1: The following equation (1) is used to compute the value of center pixel based on the value of surrounding pixel.

$$xc = \sum_{i=1}^{N} |xc - xi| \quad (1)$$

Xc = sliding window of 4 x 4 pixel
Xi = surrounding pixels
N = Pixel quantity

International Journal on Recent and Innovation Trends in Computing and Communication
ISSN: 2321-8169 Volume: 10 Issue: 2s
DOI: https://doi.org/10.17762/ijritcc.v10i2s.5927
***Article Received**: 08 October 2022 **Revised**: 12 November 2022 **Accepted**: 22 December 2022*

Step 2: The 4 × 4 sliding window is energizes inside pixel, pixels around with middle pixel are set to compute their power esteem and the middle worth comparative with the center. It will supplant the pixel in the focal point of the 4 × 4 sliding window.

Step 3: This procedure proceeds until there are no more pixels in the image.

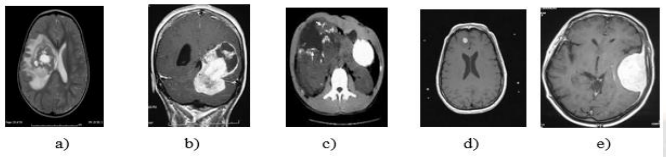

Figure 2: Input MRI images

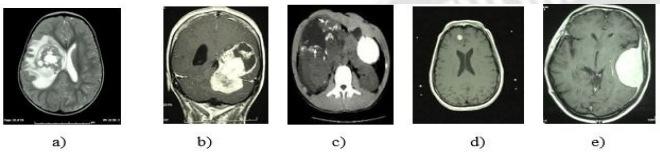

Figure 3. Result of Preprocessed MRI images

The input MRI images from BRAST database and result of preprocessed images using vectored median filter are demons red in figure 2 and figure 3. In this preprocessing result has been used for segmentation purpose

3.2 Multi-Model Clustering Segmentation

Segmentation refers to the division of a partitioned computerized image into multiple locales and the reason for division (pixel gatherings) to disentangle the processing of images that are investigated all the more seriously. The consequence of image segmentation is a gathering that by and large covers the entire image area or shape. Comparative with a similar feature (one or more), nearby areas are altogether extraordinary. The proposed strategy requires enlisting the divisions between all the data, and we accept the Euclidean partition as the principal estimation of data expels in this figuring, and in the segmentation process, the Gaussian piece is used to estimate the thickness ρi of the data point I. The following condition is used to determine the separation.

$$\delta_i = \begin{cases} min_j^{dij} p_j > p_i \\ min_j^{dij} p_j \; is \; the \; highest \; density \end{cases}$$

(2)

The novel segmentation approach might be depicted as follows, together with the portrayal of predicting the information image into shading areas and the essential idea of Multi-Model Clustering Segmentation calculation.

3.2.1 Multi-Model Clustering Segmentation - Algorithm

Step 1: Creating an element representation from the data image

Step 2: To acquire the depiction in the white mass, read the primary image data.

Step 3: Identifying the cluster centers and number

Step 4: Computing the thickness ρ and expel δ by using the equation (2). Furthermore, a while later making the decision outline given the thickness and partition

Step 5: Using the previously mentioned parameters, select information focuses with a high thickness (ρ) and a long distance (δ) as cluster habitats. After then, it's time to figure out what the group number means.

Step 6: Assigning the remaining focuses to the various groups.

Step 7: If the above two conditions are met, mark point x_i with a name that is similar to point x_i.

$$p_j > p_i$$

$$d_{ij} = min_{i\#1}^{dij}$$

Step 8: Calculate the distance (Euclidean) between each cluster and the information point.

Step 9: If the information point is closest to the cluster, leave it alone. If the information point isn't closest to its cluster, it should be moved to the closest cluster.

Step 10: Repeat the previous procedure until no information indicates moving from one cluster to the next after going through all of the information points. Now that the gatherings have stabilized, the clustering step can be completed.

Step 11: Accomplishing the last segmentation dependent on the names set apart through the last step, as appeared in Figure 5

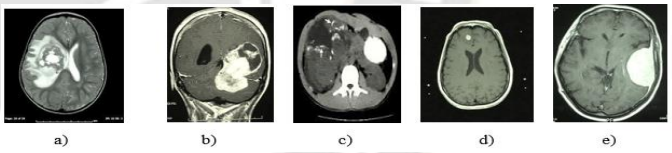

Figure 4. Preprocessed Result's Image

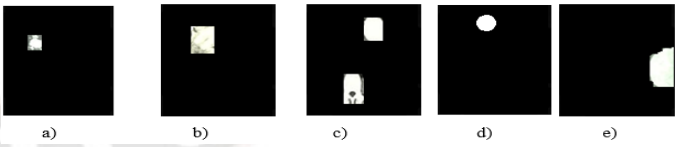

Figure 5 Result of MRI image segmentation

The figure 4 and figure 5 demonstrates the result of preprocessing and segmentation. The segmentation processed developed using multi-model clustering segmentation techniques, the result of these segmentation is used further for feature extraction and classification purpose.

3.3 Feature Extraction- Gray Level Co-occurrence Matrix (GLCM)

The GLCM is a way of pushing the practical second-order statistical system features. Relationships between pixels inside the models region by the matrix of GLCM building. The functions of GLCM is characterize an image system that

International Journal on Recent and Innovation Trends in Computing and Communication
ISSN: 2321-8169 Volume: 10 Issue: 2s
DOI: https://doi.org/10.17762/ijritcc.v10i2s.5927
***Article Received**: 08 October 2022 **Revised**: 12 November 2022 **Accepted**: 22 December 2022*

generates a Co-occurrence and then extracts the statistical operations of this matrix by calculating how often pairs of pixels occur in an image with specific values and a specific spatial relationship. The MATLAB function of GLCM is calculating, how often do calculate a pixel intensity value of i with a value of value j caused by a particular spatial relationship. The algorithm steps of feature extraction are followed.

3.3.1 Feature Extraction Algorithm

Input: Segmentation Image

Output: Extracted Feature Vectors

Process

Step 1: Noise cancelation using adaptive median filter method

Step 2: Multi-Model Clustering Segmentation

Step 3: All segmented Feature Values Fv

Fix the Diameter = Minimum Diameter of FV0;

Fix Feature Parameter Sin = Diameter *0.31

Step 4: Estimation of the Vector Features

Fix V_1 = An (FV0, Sin)

Fix V_2 = FV0 – V_1;

Step 5: For All Segmented Feature Values Fv

Fix the Feature Parameter Sout = 1.81*sin

Step 6: Estimation of the Vector Features

Fix = Dilate (FV_0, S_{out}) Fv;

SET V_3 = – FV_0;

Step 7: Return the vector values (V_1, V2& V_3).

Step 8: Compute the value of spectral zone vector feature using following equation.

$$SZFv = \int_{j=1}^{k}(V\_1 \cap V\_2 \cap V\_3) \in Ds(j)$$

The GLCM feature extraction method extracts a total of 12 different types of features, a few of which are listed below.

Energy

The energy also measures the pixel pair repeats, the textural consistency, and the second-order statistical parameter. The structure or image has the maximum energy when the distribution of grey levels in an input images is either constant or uniform.

$$Energy = \sum_{i,j=0}^{N-1}(pi,j)^2 \quad \ldots \qquad (4)$$

Where

Pij =ij[th]the normalized co-occurrence matrix entry

N = Quantity of pixels

Contrast

A measurement of contrast is the brightness differential that makes it possible to trace a value. The range is [0, 1].

$$constrast = \sum_{i,j=0}^{N-1} pi,j(i-j)^2 \quad \ldots (5)$$

Where

N-1 = Value for the total number of pixels in a dimension

Pij = Color Values.

Correlation

Correlation with a range of = [-1, 1] is used to assess the link between neighboring pixels.

$$\text{Correlation} = \frac{N\sum xy - (\sum x)(\sum y)}{\sqrt{[N\sum x^2 - (\sum x)^2][N\sum y^2 - (\sum y)^2]}} \quad \ldots (6)$$

Where:

N= Image Count

$\sum xy$= Mean value of Paired image

$\sum x$= Mean value (image x)

$\sum y$= Mean value (image y)

$\sum x^2$= Squared mean value (image x)

$\sum y^2$= Squared mean value (image y)

Homogeneity

Close to the GLCM diagonal, the component propagates homogeneity measures in the GLCM. Range= [0, 1]

$$\text{Homogeneity} = \sum_{\text{i,j=0}}^{\text{N-1}} \frac{\text{pij}}{1+(\text{i}-\text{j})^2} \ldots (7)$$

Where i, j = pixel

pij = Value of Pixel. The image acquisition begins to take place, and is taken using the vector technique not observed in the diagnostic area.

Mean

The intermediate frequency is calculated by multiplying the total number of values by the mean, which is equivalent to the sum of occurrences. The frequency of a pixel value event is only the frequency of the event frequency, whereas the frequency of a nearby pixel value is only the frequency of the event frequency.

$$Mean = \sum_{i=0}^{G-1}\sum_{j=0}^{G-1} i\, p(i,j) \ldots \qquad (8)$$

Skewness

The mean is a conditional probability used to assess the random variable, and skewness is an estimate of nonlinearity. The skewness ratio might be positive or negative, or it can be undefinable. The skewness formula is as follows:

$$Sk = \sum_{i=1}^{N} \frac{(x_i-\bar{x})^3/N}{y^3} \ldots \qquad (9)$$

Where

$\bar{x}$ = Value of Mean, y= Standard deviation Value

N = numbers of data point

Kurtosis

Height and sharpness are calculated from the total of the remainder relative proportion of a quantity termed kurtosis. High qualities have a higher, more distinct peak, whilst poor esteems have a lower, less distinct peak. As a result, chromatin

International Journal on Recent and Innovation Trends in Computing and Communication
ISSN: 2321-8169 Volume: 10 Issue: 2s
DOI: https://doi.org/10.17762/ijritcc.v10i2s.5927
***Article Received**: 08 October 2022 **Revised**: 12 November 2022 **Accepted**: 22 December 2022*

can be used to characterize more sensitive evaluations of biological pictures.

$$Ku = \frac{\sum_{i=1}^{N}(\mu_i - \mu)^4/N}{S^4} \ldots \quad (10)$$

μ = value of mean, S= Standard deviation Value

N = Numbers of data point

Standard Deviation

The phrase "standard deviation," which is defined as a variance value, refers to the intensity changes around the image's mean value. It is given by

$$SD = \sqrt{\frac{\Sigma|x-\mu|^2}{N}} \ldots\ldots \quad (11)$$

Where

x= value of image's thickness, μ = mean value

N = number of data point

Variance

The mean result of the variance p gives the variable components relatively high weights (i, j). It refers to the pixel pairs' grey level variability as well as the polynomial computation. It is given by

$$Var = \sum_{i=0}^{G-1}\sum_{j=0}^{G-1}(i-\mu)^2\, p(i,j) \ldots (12)$$

3.4 Convolutional Gated Recurrent Neural Network (CGRNN)

A CGRNN is a deep learning framework that is produced for ceaseless information processing. It has neural networks that forward the circular associations of the stream.

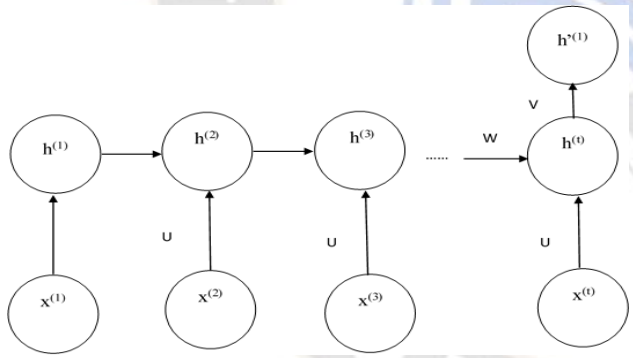

Figure 6 Convolutional Gated Recurrent Neural Network

A basic CG_RNN architecture is shown in Figure 6. In the figure, every node speaks to a layer of network at the point unfailingly. It contains hidden layer input (U), hidden to the hidden layer (W) and hidden to output layer (V).The last weight matrix is then gone through a softmax capacity to create a numeric Y esteem that orders Ŷ as a paired variable. The misfortune work is then used to think about the Y-real worth and Y-anticipated (Ŷ) esteem. In any case, there is no issue with the current CG_RNN providing input suggestions to the network output layer and along these lines on network output.

In this way, two mainstream arrangements have been grown: Gated Recurrent Unit (GRU) and Long Short-Term Memory (LSTM). In this exploration, CG_RNN-LSTM design is deployed. Blocks comprise of at any rate one independent collector cell with various increase units, for example, the info entryway, overlook door, and yield door. The data is put away and countersigned as 0 and 1. Dropout is used to reduce overflow. A regularization technique is used to provide access to the gates through the reservation.

3.4.1 CGRNN Algorithm

Step1: The forward spread of an arrangement configuration's contribution by methods for the CGRNN with a positive ultimate objective to create the proliferation's yield activations.

Step2: The back proliferation of the engendering's yield incitations by methods for the CGRNN utilizing the arrangement configuration's concentration as a piece of the solicitation to produce the deltas of the whole yield and hidden neurons

Step3: Increment its yield delta and data, actuation to accomplish the slope of the weight.

Step4: Take the weight in the reverse way of the angle by removing a portion of it from the weight.

Step5: The learning rate is a measure of how much something impacts the speed and character of learning.

Step6: The slant of a weight picture where poor behavior is going upward, which is why the weight bears need to be renewed in the other direction.

In this research, the brain tumor was tested for classification. The CG-RNN model is also demonstrated using the MATLAB programming language. Accuracy, specificity and sensitivity are utilized to assess the proposed nonlinear vector execution of the degenerative neural network framework. These parameters are estimated through tangle lab reenactment with the reaction following parameters

a. Ratio of True Positive (TP) b. Ratio of True Negative (TN) c. Ratio of False Positive (FP) d. Ratio False Negative (FN).

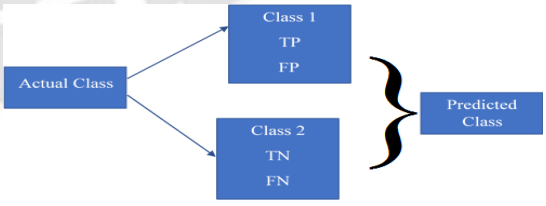

Figure 7 Confusion matrix

Confusion matrix block diagram shown in Figure 7. In this figure clearly states that it have two classes, such as class1 (TP and FP) and class2 (TN and FN). A significant issue that must be tended to in approving a programmed technique for brain tumor classification methods through which the classification is quantitatively evaluated. From the confusion

International Journal on Recent and Innovation Trends in Computing and Communication
ISSN: 2321-8169 Volume: 10 Issue: 2s
DOI: https://doi.org/10.17762/ijritcc.v10i2s.5927
***Article Received**: 08 October 2022 **Revised**: 12 November 2022 **Accepted**: 22 December 2022*

matrix figure 6, the accuracy, sensitivity and specificity are measured using equation 13, 14 and 15 respectively.

Accuracy: It is the level of closeness for estimations of an amount to that amount's actual esteem. It is given as

$$\text{Accuracy} = {}^{TP+TN}/_{TP+FP+TN+FN} \quad \ldots\ldots \quad (13)$$

Sensitivity: It gauges the extent of negatives which are effectively recognized. It is spoken to as

$$\text{Sensitivity} = {}^{TP}/_{TP+FP} \quad (14)$$

Specificity: It is characterized as the portion of the classified picture, which is applicable to the expectations. It is given as

$$\text{Specificity} = {}^{TN}/_{TN+TP} \quad (15)$$

IV. Results And Discussion

The functions of simulation result for proposed MRI brain tumor detection and classification system are evaluated using BRAST 2015 database (which may contain 338 images) is discussed for this section. The simulation is developed using matlab Simulink software. The obtained **GLCM** features are fed to the Convolutional Gated Recurrent Neural Network model for each class, and these models has used the features with 70% of the training and 30% of the testing. The figure 8 demonstrates the simulation model of proposed CGRNN based brain tumor analyzing system.

The figure 9 and table 1 discuss the simulation results of feature extraction using GLCM feature extraction method for five different types of. In these extracted features are further trained to CGRNN classifier to classify the tumor types. The obtained classification results are compared with existing methods (shown in Table 2) using the response of confusion matrix values (TN, FN, TP & FP).

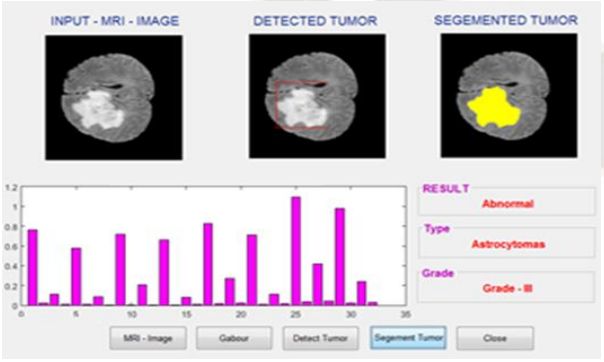

Figure 8: Snapshot for tumor detected area from the MRI image – convolutional gated recurrent neural network

Table 1 GLCM feature extraction for MRI tumor detection and classification

Features					
Mean	0.0036	0.0045	0.0014	0.0040	0.0037
Standard Deviation	0.0897	0.0896	0.0898	0.0897	0.0897
Entropy	2.7732	2.3280	2.8901	2.1047	2.8414
RMS	0.08980	0.0898	0.0898	0.0898	0.0898
Variance	0.0079	0.0080	0.0080	0.0080	0.0079
Smoothness	0.9307	0.9441	0.8416	0.9374	0.9330
Kurtosis	13.5553	11.8567	9.2548	13.1205	12.5895
Skewness	1.3933	1.0823	0.6803	1.1019	1.0199
IDM	1.10638	0.13569	0.4306	0.2127	0.6466
Contrast	0.3245	0.2700	0.2391	0.2919	0.2992
correlation	0.1530	0.01845	0.2057	0.1775	0.0920
Energy	0.7633	0.7667	0.7903	0.8037	0.7890
Homogeneity	0.9318	0.9353	0.9401	0.9438	0.9393

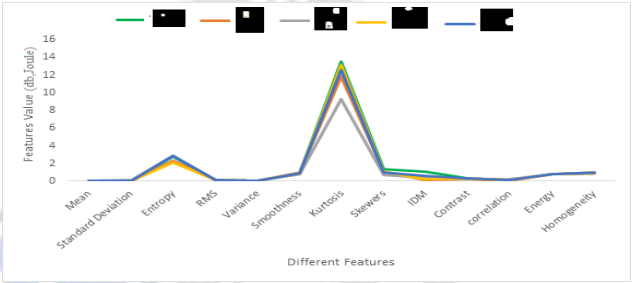

Figure 9. Analysis of Feature Extraction

Table 2 Analysis of MRI brain Tumor classification ratio

Methods	Sensitivity (%)	Specificity (%)	Classification Accuracy (%)	Positive Predictive Value (%)	Negative Predictive Value (%)	FDR (%)
SVM	96.30	83.72	90.72	88.14	94.74	31.3
SVM-PSO	96.29	89.34	95.87	96.29	95.34	28.3
CGRNN	97.30	96.54	98.45	98.6	94.5	

The performance Analysis classification ratio of proposed Convolutional Gated Recurrent Neural Network method with existing SVM and SVM- PSO methods based MRI brain tumor classification system is shown in Figure 10 and table 2 respectively.

The Analysis of Tumor classification ratio for proposed convolutional Gated Recurrent Neural Network method with existing method based MRI brain tumor detection system is shown in Table 2. In this compression clearly states that the proposed CGRNN system achieves significant result as compared with existing SVM and SM-PSO methods. The sensitivity, specificity and accuracy of CGRNN are 97.30%, 96.54% and 98.45% respectively.

International Journal on Recent and Innovation Trends in Computing and Communication
ISSN: 2321-8169 Volume: 10 Issue: 2s
DOI: https://doi.org/10.17762/ijritcc.v10i2s.5927
***Article Received**: 08 October 2022 **Revised**: 12 November 2022 **Accepted**: 22 December 2022*

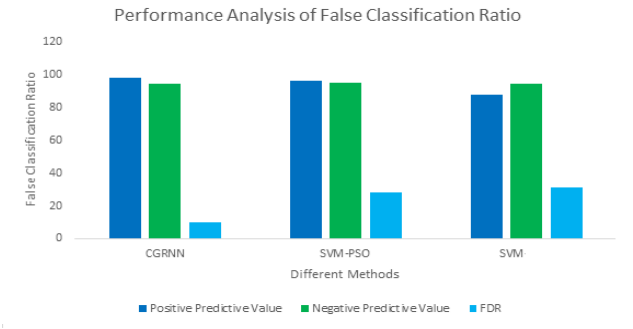

Figure 10 Analysis of MRI brain Tumor False classification ratio

In this compression clearly states that the proposed CGRNN method achieves perfect result as compared with existing SVM and SM-PSO methods. The Ratio of Positive predictive, Negative Predictive and False Detection Ratio of the proposed CGRNN are 98.60%, 94.50% and 10.20% respectively.

V. Conclusion

This work introduced a CGRNN method for tumor detection and classification from MRI images. A significant amount of this MRI image of the brain tumor division strategy is due to the non-invasive and great subtle tissue differentiation and utilization of MRI grouping and the use of different highlights in nearby neighbors, and considering spatial data clustering techniques. This also gives a strong result within a reasonable calculation time. Finally, CGRNN classifiers have been used to recognize different types of brain cancer. The proposed system was found to be efficient in classifying these samples and answered any anomalies. The whole system is divided into two stages, the first learning / training stage and the second recognition / testing stage. The proposed CGRNN method achieves the best results as compared with existing SVM and SM-PSO methods. In future, a deep learning method is used to improve the overall performance of MRI brain tumor detection and classification.

References

[1] Louis, D. N.; Perry, A.; Reifenberger, G.; von Deimling, A.; Figarella-Branger, D.; Cavenee, W. K.; Ohgaki, H.; Wiestler, O. D.; Kleihues, P.; Ellison, D. W. The 2016 world health organization classification of tumors of the central nervous system: A summary. ActaNeuropathologica Vol. 131, No. 6, 803–820, 2016.

[2] Menze, B.; Reyes, M.; van Leemput, K. The multimodal brain tumorimage segmentation benchmark (BRATS). IEEE Transactions on Medical Imaging Vol. 34, No. 10, 1993–2024, 2015.

[3] Robles, M.; Aparici, F.; Mart´ı-Bonmat´ı, L.; Garc´ıaG´omez, J. M. Automated glioblastoma segmentation based on a multiparametric structured unsupervised classification. PLoS ONE Vol. 10, No. 5, e0125143, 2015.

[4] Bauer, S.; Wiest, R.; Nolte, L. P.; Reyes, M. A survey of MRI-based medical image analysis for brain tumor studies. Physics in Medicine and Biology Vol. 58, No. 13, R97–R129, 2013.

[5] Havaei, M.; Davy, A.; Warde-Farley, D.; Biard, A.; Courville, A.; Bengio, Y.; Pal, C.; Jodoin, P. M.; Larochelle, H. Brain tumor segmentation with deep neural networks. Medical Image Analysis Vol. 35, 18– 31, 2017.

[6] A deep convolutional encoder-decoder architecture for image segmentation. IEEE Transactions on Pattern Analysis and Machine Intelligence Vol. 39, No. 12, 2481– 2495, 2017.

[7] Noh, H.; Hong, S.; Han, B. Learning deconvolution network for semantic segmentation. In: Proceedings of the IEEE International Conference on Computer Vision, 1520–1528, 2015.

[8] Bakas, S.; Akbari, H.; Sotiras, A.; Bilello, M.; Rozycki, M.; Kirby, J. S.; Freymann, J. B.; Farahani, K.; Davatzikos, C. Advancing the cancer genome atlas glioma MRI collections with expert segmentation labels and radiomic features. Scientific Data Vol. 4, 170117, 2017

[9] yang, G.; Nawaz, T.; Barrick, T.R.; Howe, F.A.; Slabaugh, G. Discrete wavelet transform-based whole-spectral and subspectral analysis for improved brain tumor clustering using single voxel MR spectroscopy. IEEE Trans. Biomed. Eng. 2015, 62, 2860–2866.

[10] Mittal, M.; Goyal, L.M.; Kaur, S.; Kaur, I.; Verma, A.; Hemanth, D.J. Deep learning based enhanced tumor segmentation approach for MR brain images. Appl. Soft Comput. 2019, 78, 346–354.

[11] Reza, S.; Iftekharuddin, K.M. Improved brain tumor tissue segmentation using texture features. In Proceedings of the MICCAI BraTS (Brain Tumor Segmentation Challenge), Boston, MA, USA, 14 September 2014; pp. 27–30.

[12] Kleesiek, J.; Biller, A.; Urban, G.; Kothe, U.; Bendszus, M.; Hamprecht, F. Ilastik for multi-modal brain tumor segmentation. In Proceedings of the MICCAI BraTS (Brain Tumor Segmentation Challenge), Boston, MA, USA, 14 September 2014; pp. 12–17

[13] Long, J.; Shelhamer, E.; Darrell, T. Fully convolutional networks for semantic segmentation. In Proceedings of the IEEE Conference on Computer Vision and Pattern Recognition, Boston, MA, USA, 7–12 June 2015; pp. 3431–3440.

[14] Zheng, S.; Jayasumana, S.; Romera-Paredes, B.; Vineet, V.; Su, Z.; Du, D.; Torr, P.H. Conditional random fields as recurrent neural networks. In Proceedings of the IEEE International Conference on Computer Vision, Santiago, Chile, 7–13 December 2015; pp. 1529–1537.

[15] Liu, Z.; Li, X.; Luo, P.; Loy, C.-C.; Tang, X. Semantic image segmentation via deep parsing network. In Proceedings of the IEEE International Conference on Computer Vision, Santiago, Chile, 7–13 December 2015; pp. 1377–1385.

International Journal on Recent and Innovation Trends in Computing and Communication
ISSN: 2321-8169 Volume: 10 Issue: 2s
DOI: https://doi.org/10.17762/ijritcc.v10i2s.5927
***Article Received**: 08 October 2022 **Revised**: 12 November 2022 **Accepted**: 22 December 2022*

[16] Wang, G.; Zuluaga, M.A.; Pratt, R.; Aertsen, M.; Doel, T.; Klusmann, M.; Ourselin, S. Slic-Seg: A minimally interactive segmentation of the placenta from sparse and motion-corrupted fetal MRI in multiple views. Med. Image Anal. 2016, 34, 137–147.

[17] Top, A.; Hamarneh, G.; Abugharbieh, R. Active learning for interactive 3D image segmentation. In International Conference on Medical Image Computing and Computer-Assisted Intervention; Springer: Berlin, Germany, 2011; pp. 603–610

[18] Havaei, M.; Davy, A.; Warde-Farley, D.; Biard, A.; Courville, A.; Bengio, Y.; Larochelle, H. Brain tumor segmentation with deep neural networks. Med. Image Anal. 2017, 35, 18–31.

[19] Pereira, S.; Pinto, A.; Alves, V.; Silva, C.A. Deep convolutional neural networks for the segmentation of gliomas in multi-sequence MRI. BrainLes 2015, 2015, 131–143.

[20] Kamnitsas, K.; Ledig, C.; Newcombe, V.F.; Simpson, J.P.; Kane, A.D.; Menon, D.K.; Glocker, B. Efficient multi-scale 3D CNN with fully connected CRF for accurate brain lesion segmentation. Med. Image Anal. 2017, 36, 61–78.

[21] Pereira, S.; Pinto, A.; Alves, V.; Silva, C.A. Brain tumor segmentation using convolutional neural networks in MRI images. IEEE Trans. Med. Imaging 2016, 35, 1240–1251.

[22] Cheng, J.; Huang, W.; Cao, S.; Yang, R.; Yang, W.; Yun, Z.; Feng, Q. Enhanced performance of brain tumor classification via tumor region augmentation and partition. PLoS ONE 2015, 10, e0140381.

[23] Wang, R.; Ma, J.; Niu, G.; Zheng, J.; Liu, Z.; Du, Y.; Yang, J. Differentiation between solitary cerebral metastasis and astrocytoma on the basis of subventricular zone involvement on magnetic resonance imaging. PLoS ONE 2015, 10, e0133480.